

I.V. Semkiv¹, H.A. Ilchuk¹, N.Y. Kashuba¹, V.M. Kordan², A.I. Kashuba¹

Synthesis, Crystal and Energy Structure of the Ag₈SnS₆ Crystal

¹Lviv Polytechnic National University, Lviv, Ukraine, igor.v.semkiv@lpnu.ua

²Ivan Franko National University of Lviv, Lviv, Ukraine

The Ag₈SnS₆ crystal was synthesized by directly melting a high-purity stoichiometric mixture of elementary Ag, Sn, and S in a sealed quartz ampoule. This argyrodite crystallizes in the orthorhombic structure (*Pna*2₁ space group (No. 33)) at room temperature. The electronic band structure and density of states of an α''-Ag₈SnS₆ crystal are evaluated theoretically using the generalized gradient approximation (GGA) and local density approximation (LDA) in first-principle calculations. A Perdew–Burke–Ernzerhof functional (PBE) and (PBEsol) were utilized for GGA calculation. All calculated parameters correlate well with known experimental data. The calculation of the effective mass of electrons and holes was performed based on the electronic band structure. The anisotropic behavior of electronic band structure is discussed.

Keywords: argyrodite, synthesis, X-ray diffraction, morphology, density functional theory, band structure, effective mass, the density of states.

Received 18 May 2023; Accepted 26 August 2023.

Introduction

The argyrodite family [1] has a great variety of compounds and is characterized by the general formula (A⁺)_{12–n}Bⁿ⁺(X^{2–})₆ (with A⁺ = Li⁺, Cu⁺, Ag⁺; Bⁿ⁺ = Ga³⁺, Si⁴⁺, Ge⁴⁺, Sn⁴⁺, P⁵⁺, As⁵⁺; X^{2–} = S^{2–}, Se^{2–}, Te^{2–}). These compounds are actively studied for potential use in photovoltaic [2–4], thermoelectricity [5], nonlinear optic [6], solid-state batteries [7], hydrogen generation [8], etc. Argyrodites are characterized by a tetrahedrally close-packed polyanionic structure with weakly bound Ag/Cu cations, allowing certain phonon and electronic transport manipulations for their practical use, for example, in thermoelectricity [5].

The Ag₈SnS₆ compound is formed from the melt at 1125 K [9] (1112 K [10]) and undergoes one polymorphic transformation [10]. The structure of low temperature (LT) Ag₈SnS₆ (α''-modification) is orthorhombic: space group *Pna*2₁, *a* = 1.5298 nm, *b* = 0.7548 nm, *c* = 1.0699 nm [9, 11], and high temperature (HT) Ag₈SnS₆ (γ-modification) is cubic: space group *F*-43*m*, *a* = 1.085 nm [10]. The structural transition between the cubic (γ) and orthorhombic (α'') phases occurs at 455 K [5].

The literature presented certain studies of the electronic characteristics of Ag₈SnS₆ argyrodite. In [12] the electronic and optical properties are investigated using density functional theory (DFT) with both GGA (generalized gradient approximation) and LDA (local density approximation). The Monkhorst–Pack **k**-points grid sampling was set at (2×4×2) points for the first Brillouin zone (BZ). The obtained band gap is about 0.58 eV, which is less than the experimental value of 1.39 eV. Dielectric function, absorption spectrum, and refractive index are also calculated. The static refractive index *n*₀ of polycrystalline Ag₈SnS₆ is 2.04 [12]. Ref [6] presents the calculation of the electronic structure and optical properties by the DFT with GGA and Perdew–Burke–Ernzerhof (PBE) functional and the norm-conserving pseudopotential. BZ was performed using a (2×4×3) Monkhorst–Pack **k**-point. The obtained band gap is about 0.55 eV in [6]. The birefringences are 0.095 for Ag₈SnS₆ at 1064 nm [6]. A similar calculation was also performed by [13]. In literature presented lattice dynamics calculations of 2×1×1 supercell structures of Ag₈SnS₆, each of which contains 120 atoms and was sampled with a 2×3×2 Γ -centered **k**-point grid. The calculations of phonon structure confirm the rattling-like, low-lying

optical modes and weakly bounded behavior of Ag atoms [13]. The density of states for Ag_8SnS_6 in the LT structure ($Pna2_1$) was computed using density functional theory (DFT), and presented in reference [14]. The calculation was performed by DFT with PBEsol exchange-correlation functional, with projected augmented wave (PAW) method and Monkhorst-Pack \mathbf{k} -point grid of $(6 \times 6 \times 4)$ and $(3 \times 6 \times 4)$ [14]. In [15], a similar approach was employed to calculate the band structure of Ag_8SnS_6 , except an additional modified Becke-Johnson (mBJ) exchange potential correction. The calculation utilized two hundred sixteen independent \mathbf{k} points on a grid of $8 \times 17 \times 12$ lattice points. The resulting band gap was determined to be 1.3 eV [15].

The main objective of this study is to investigate the synthesis and crystal structure of the α' - Ag_8SnS_6 crystal. Additionally, the electronic structure and density of states of the crystal will be calculated and analyzed. The effective mass of electrons and holes in α' - Ag_8SnS_6 crystal was calculated based on the electron energy structure.

I. Experimental details

The argyrodite compound Ag_8SnS_6 was synthesized by direct melting of a stoichiometric mixture of high purity (>99 %) elemental silver (Ag), tin (Sn), and sulfur (S) in an evacuated (10^{-5} Torr) quartz ampoule. The synthesis was carried out in a single-zone furnace equipped with elements of rotation and vibration of the sample. The temperature regimes of the synthesis were chosen based on the analysis of phase diagrams of the compound and other studies presented in the literature [13–20]. The ampoule was heated at a rate of 50 K to 1250 K with intermediate exposures at a constant temperature for the reactions of elemental sulfur melting, formation of binary compounds of sulfur with elemental silver and tin, and passing of the reaction between binary compounds Ag_2S and SnS_2 with the formation of Ag_8SnS_6 argyrodite. To ensure the homogeneity of the compound, after reaching 1250 K, the melt was kept at a constant temperature for 60 hours. The sample was then cooled to room temperature at a constant rate except for the phase

transition region where cooling occurred more slowly to avoid the destruction during phase change.

The phase analysis and crystal structure refinement of Ag_8SnS_6 was examined with X-ray diffraction data (XRD) obtained on DRON-2.0M diffractometer at room temperature with the $K\alpha$ radiation ($\lambda = 1.936087 \text{ \AA}$) of Fe. The surface morphology of the crystal was studied using a Tescan VEGA 3 LMU scanning electron microscope (SEM) equipped with an energy-dispersive X-ray analyzer (Oxford Instruments Aztec ONE with a detector of the X-MaxN20).

II. Calculation details

Theoretical calculations in this study were conducted using the density functional theory (DFT) approach. To calculate the electron band structure of α' - Ag_8SnS_6 , the crystal structure and lattice parameters were obtained from X-ray diffraction (XRD) data taken at room temperature. To characterize the exchange-correlation energy of the electronic subsystem, functional in the approximation of local density (LDA) and generalized gradient (GGA) was used. For GGA calculation was used two parameterizations of the Perdew–Burke–Ernzerhof (PBE [21] and PBEsol – for solids [22]).

The value of the energy of cutting-off ($E_{\text{cut-off}}$) the plane waves is listed in Table 2. This value corresponds to the minimum of total energy (E_{total}), which is listed in Table 2, too. The integration over the BZ was performed on the $1 \times 2 \times 1$ grid of \mathbf{k} points using the Monkhorst–Pack scheme [23]. The energy band diagram was constructed using specific points in the Brillouin zone (BZ) in reciprocal space. The chosen points and their corresponding coordinates are as follows: $\Gamma(0, 0, 0)$, $X(0, 0.5, 0)$, $Y(-0.5, 0, 0)$, $Z(0, 0, 0.5)$, $S(-0.5, 0.5, 0)$, $T(-0.5, 0, 0.5)$, $U(0, 0.5, 0.5)$ and $R(-0.5, 0.5, 0.5)$.

III. Results and Discussion

3.1. Crystal structure

The Ag_8SnS_6 crystal structure was determined using X-ray diffraction (XRD) analysis. The XRD (see Fig. 1)

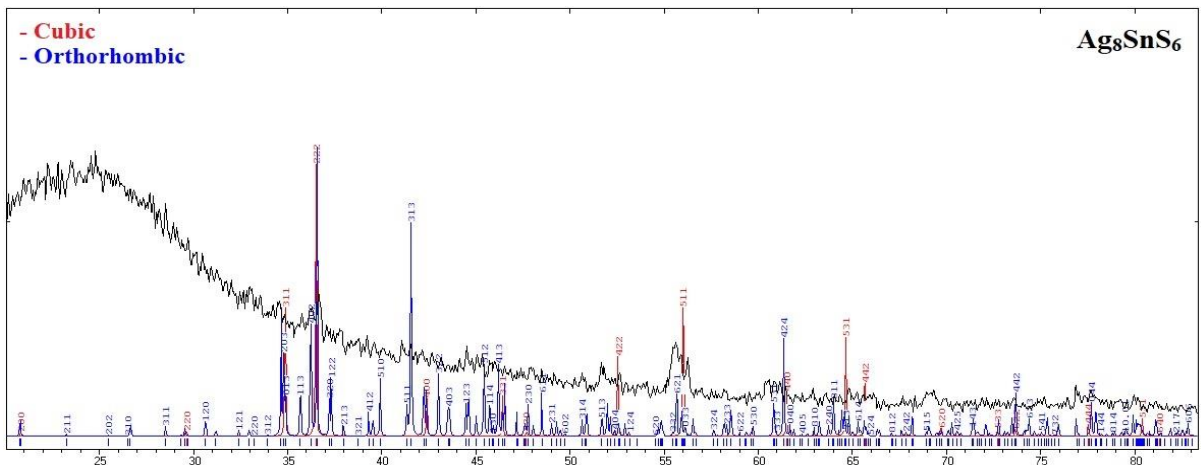


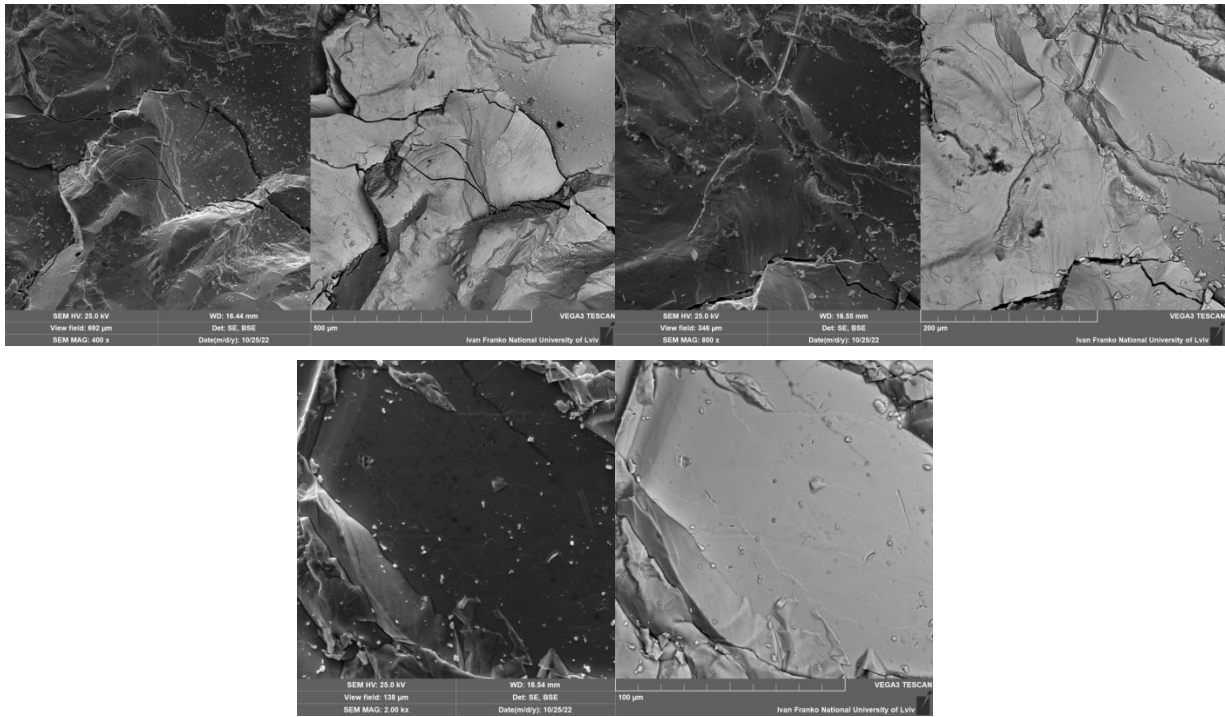
Fig. 1. Measured and calculated XRD patterns for Ag_8SnS_6 crystal (Fe $K\alpha$ radiation). Experimental data – black line, calculated data – red and blue line (detail on the legend to figure).

Table 1

 Structural data for Ag_8SnS_6 crystal at room temperature

Method	a , Å	b , Å	c , Å	V , Å ³	Reference
XRD	15.298(3)	7.552(2)	10.719(3)	1238.6(3)	This work
XRD	15.298	7.548	10.699	–	[26]
–	15.2980	7.5480	10.6990	1235.41	[12]
GGA+PBE	15.4883	7.65393	10.8697	1288.56	[12]
GGA+PBE	15.492716	7.661063	10.868171	1289.95	This work
XRD*	10.711(2)	–	–	1229.1(8)	This work

*for the unidentified impurity cubic phase


Fig. 2. SEM image of α'' - Ag_8SnS_6 crystal.

shows that the Ag_8SnS_6 crystal has a large amorphous contribution. This material crystallizes in two different crystal structure modifications (α'' and γ). The α'' - Ag_8SnS_6 modification belongs to the orthorhombic structure ($Pna2_1$ space group [24, 25]). High-temperature γ -phase Ag_8SnS_6 crystallizes in a cubic structure with the $F-43m$ space group [24, 25]. The temperature of the structural transition (from orthorhombic to cubic structure) between these modifications of the Ag_8SnS_6 argyrodite is equal to 445 K [24, 25]. Two theoretical XRD patterns were used (for orthorhombic and cubic crystal structures) for the identification of the crystal structure and lattice parameters of the studied crystal.

Based on the XRD data, we obtained the crystal structure of the Ag_8SnS_6 crystal corresponding to the orthorhombic structure ($Pna2_1$ space group) with lattice parameters listed in Table 1. As a result, we obtained α'' -modification of the Ag_8SnS_6 crystal at room temperature. However, we need to note that the sample presents a small amount of the impurities phase of the cubic structure. The lattice parameters of the unidentified impurity cubic phase were listed in Table 1.

3.2. Morphology analysis

The morphology of the Ag_8SnS_6 crystal was investigated by SEM. The surface morphology of the α'' - Ag_8SnS_6 crystal shows small agglomeration and cracks (see Fig. 2). Energy dispersive X-ray spectrometry was used to confirm the elemental composition of the sample (Fig. 3). The quantitative result gives the atomic ratio of 63.97:1.66:34.38 for Ag:Sn:S, which is close to the ideal value of 8:1:6 in Ag_8SnS_6 .

3.3. Analysis of the electron band energy structure

As quoted in the second section of this work, electron energy band structure was calculated using three methods (LDA, GGA+PBE and GGA+PBEsol). The bandgap (E_g) near 0.5 eV was observed for all calculation methods (see Table 2), which is lower than the experimentally measured $E_g = 1.39$ eV [12]. The same situation is realized in Ref. [12].

The underestimation of the bandgap value is often observed with this calculation approach using. A technique called the 'scissor' operator (ΔE) is commonly employed to align the results closer to experimental

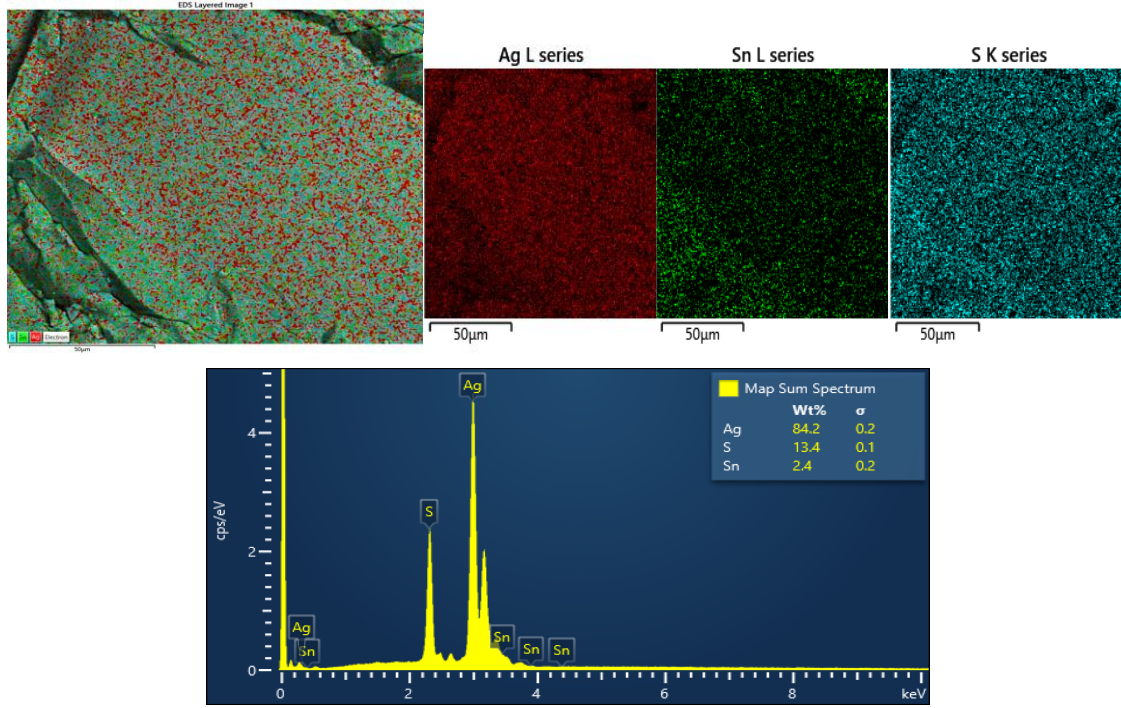


Fig. 3. Energy dispersion of X-rays analysis of α'' - Ag_8SnS_6 crystal.

Table 2

Energy properties for Ag_8SnS_6 crystal

Method	E_g^{dir} , eV	ΔE , eV	$E_{\text{cut-off}}$, eV	E_{total} , keV	m_e^*/m_0	m_h^*/m_0
LDA	0.506	0.884	800	-133.553	0.780	-6.546
GGA+PBE	0.534	0.856	850	-133.572	0.806	-6.796
GGA+PBEsol	0.449	0.941	850	-133.427	0.809	-6.487

values. This operator shifts the conduction band to higher energy regions, effectively altering the bandgap [27, 28]. The adjustment is based on the similarity between the $E(\mathbf{k})$ dispersion dependencies of conduction band energies derived from the Kohn-Sham equations [29]. The 'scissor' operator is applied by shifting the calculated conduction bands until the experimental value of the minimum energy gap (E_g) of the crystal is attained [27]. The specific values used for the 'scissor' operator are listed in Table 2. However, it's important to note that this adjustment does not significantly impact the overall electronic and structural properties trends, as evidenced by previous calculations of electronic states [27, 28, 30-32].

A higher correlation between obtained value of the bandgap and experimental data is observed for the GGA+PBE method. As a result, this article provides electron energy band structure and density of states (DOS, see below) calculated using the GGA+PBE method. Calculated lattice parameters were listed in Table 1.

In Fig. 4, the energy band diagrams of the α'' - Ag_8SnS_6 crystal are depicted along the highly symmetric lines of the Brillouin zone (BZ). The energy levels are measured with respect to the Fermi level, represented by the red line in Fig. 4. The analysis of the theoretical calculations reveals that the smallest bandgap is located at the center of the Brillouin zone, specifically at the point Γ . This indicates that the crystal possesses a direct energy band gap (E_g^{dir}).

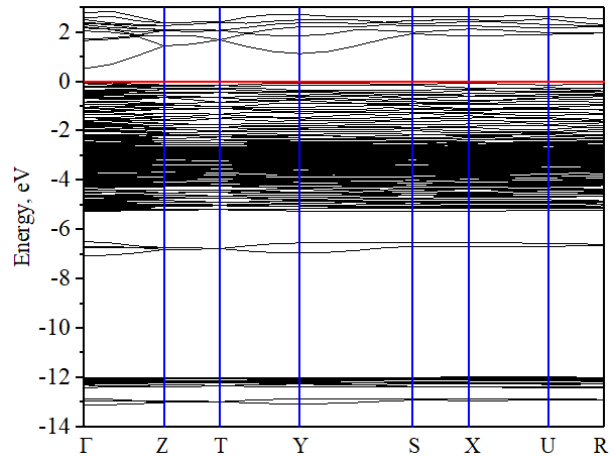


Fig. 4. Calculated electron band energy structure of α'' - Ag_8SnS_6 crystal using the GGA+PBE method.

Also, we can see from Fig. 4 a clear anisotropy difference $E(\mathbf{k})$ between the valence and conduction bands. The valence complex top is flatter, which is explained by the fact that holes are less mobile than electrons. This behavior is caused by the inverse relationship between the effective mass (m^*) of the electron (m_e^*)/hole (m_h^*) and the spread $E(\mathbf{k})$ of energy levels [28]:

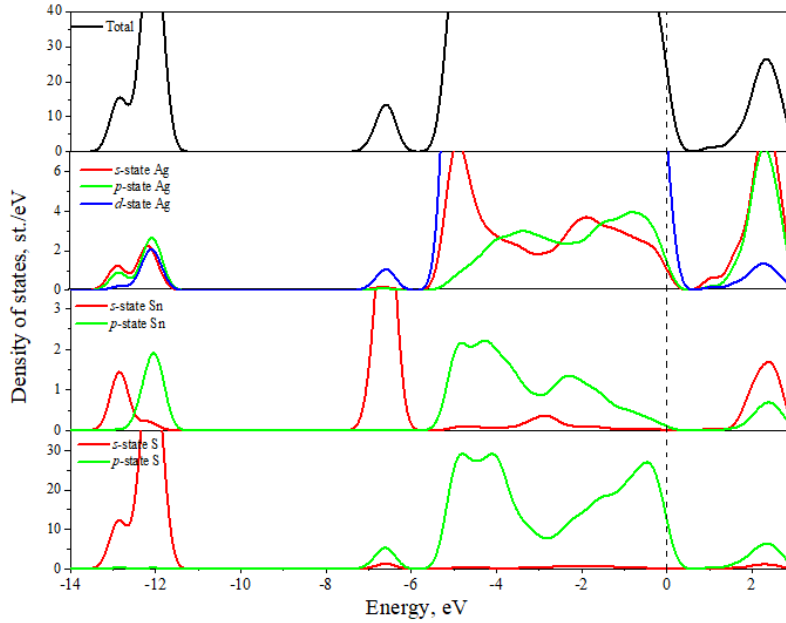


Fig. 5. Calculated electron density of states of α'' - Ag_8SnS_6 crystal using the GGA+PBE method.

$$\frac{1}{m^*} = \frac{4\pi^2}{h^2} \frac{d^2 E(\mathbf{k})}{dk^2}. \quad (1)$$

where h – the Planck constant, $E(\mathbf{k})$ – dependence of the band energy E on the electron wave vector \mathbf{k} . As a result, we can see that the maximum dispersion of valence and conduction bands was observed for $\Gamma \rightarrow Z$ direction (the same situation in the $Y \rightarrow T$ direction). The electrons and holes effective masses in α'' - Ag_8SnS_6 crystal have been calculated by employing the Effective Mass Calculator [33]. The calculated effective masses for α'' - Ag_8SnS_6 crystal are presented in Table 2. The resultant absolute value of the $|m^*|$ for the conduction band ($\sim 0.8 m_0$) is lower than that for the valence band ($\sim 6 m_0$).

3.4. Analysis of the electron density of states

By analyzing the partial contributions of individual levels to the total density of states (DOS) and the contributions of individual bands to the electronic density, the origins of the valence and conduction bands in the α'' - Ag_8SnS_6 crystal can be identified. Fig. 5 illustrates this analysis, providing insights into the specific bands and energy levels that contribute to the electronic properties of the crystal.

The lowest energy bands lying in the range from -14 to -12 eV are formed by s -electronic states of S. The formation of subsequent bands that are spread from -7 to -6 eV and the energy marker comes from the contribution of the s -electronic states of Sn. The top of the valence band is composed of the d -electronic states of Ag, with some ‘admixture’ of the p -electronic states of Ag and S. On the other hand, the bottom of the conduction band is mainly composed of the s - and p -electronic states of Ag.

This mainly is caused by the highest relative content of argyrodite and sulfur atoms in α'' - Ag_8SnS_6 . The smallest partial DOS of tin is explained by the smaller content in the formula unit α'' - Ag_8SnS_6 . We assume that the direct-bandgap transition (localized at the point Γ of the BZ) can be formed by the Ag–S links.

The band structure of the α'' - Ag_8SnS_6 crystal exhibits a significant hybridization of electronic states near the energy gap (E_g). This is evident from the similar maxima in the partial density of states (DOS) within the energy range from the top of the valence to the bottom of conduction bands, as shown in Fig. 4. This observation suggests that the electronic states primarily originate from the bonding electrons of the most numerous atoms, such as silver (argyrodite) and sulfur. This hybridization and contribution of these atoms to the electronic states are likely to play a crucial role in the electron conductivity characteristics of α'' - Ag_8SnS_6 .

Conclusion

In this work, the crystal and electronic structure of the α'' - Ag_8SnS_6 crystal have been studied. The main results obtained by us can be summarized in brief as follows.

The Ag_8SnS_6 crystal was synthesized and grown and its X-ray-based crystal structure was studied. The lattice parameters $a = 15.298(3) \text{ \AA}$, $b = 7.552(2) \text{ \AA}$, $c = 10.719(3) \text{ \AA}$, $V = 1238.6(3) \text{ \AA}^3$, $Pna2_1$ space group (No. 33) for α'' - Ag_8SnS_6 crystal were refined and showed good correlation with known literature data. XRD analysis showed impurities with cubic crystal structure in the sample. We do not reject the possibility of binary impurities in the sample.

The electronic energy spectrum of the α'' - Ag_8SnS_6 crystal was investigated through first-principle theoretical studies using the reliable techniques of DFT. In these studies, various approximations were employed, including the LDA, GGA+PBEsol, and GGA+PBE. The GGA+PBE method showed a higher correlation of obtained value of the bandgap with experimental data. It was established that the smallest bandgap in the electronic energy spectrum of the α'' - Ag_8SnS_6 crystal is situated at the center of the Brillouin zone, specifically at the Γ point. Therefore, our argyrodite should reveal direct optical transitions. The direct-bandgap transition (localized at the

point Γ of the BZ) can be formed by the Ag–S links. The band structure of the α'' -Ag₈SnS₆ crystal exhibits a significant hybridization of electronic states in the energy ranges near the energy gap (E_g). The effective mass of the electron ($\sim 0.8m_0$) and hole ($\sim 6m_0$) was calculated based on results of the electronic structure. Dispersion behaviors of electron energy level are discussed based on results of effective mass.

Acknowledgments

This work was supported by the Project of Young Scientists 0123U100599 of the Ministry of Education and

Science of Ukraine.

Semkiv I.V. – Ph.D., Head of Department of General Physics;

Ilchuk H.A. – Sc.D., Professor at the Department of General Physics;

Kashuba N.Y. – Engineer at the Department of General Physics;

Kordan V.M. – Ph.D., Research Fellow at the Department of Inorganic Chemistry;

Kashuba A.I. – Ph.D., Doctoral Student at the Department of General Physics.

- [1] W.F. Kuhs, R. Nitsche, K. Scheunemann, *The argyrodites — A new family of tetrahedrally close-packed structures*, Mater. Res. Bull., 14(2), 241 (1979); [https://doi.org/10.1016/0025-5408\(79\)90125-9](https://doi.org/10.1016/0025-5408(79)90125-9).
- [2] B. Zhou, Y. Xing, S. Miao, M. Li, W.-H. Zhang, C. Li, *Synthesis and Characterization of Ag₈(Ge_{1-x}Sn_x)(S_{6-y}Se_y) Colloidal Nanocrystals*, Chem. Eur. J., 20, 12426 (2014); <http://dx.doi.org/10.1002/chem.201404220>.
- [3] Q. He, T. Qian, J. Zai, Q. Qiao, S. Huang, Y. Li, M. Wang, *Efficient Ag₈GeS₆ counter electrode prepared from nanocrystal ink for dye-sensitized solar cells*, J. Mater. Chem. A., 3, 20359 (2015). <https://doi.org/10.1039/C5TA05304H>.
- [4] Q. He, S. Huang, C. Wang, Q. Qiao, N. Liang, M. Xu, W. Chen, J. Zai, X. Qian, *The Role of Mott–Schottky Heterojunctions in Ag–Ag₈SnS₆ as Counter Electrodes in Dye-Sensitized Solar Cells*, ChemSusChem., 8(5), 817 (2015); <https://doi.org/10.1002/cssc.201403343>.
- [5] S. Lin, W. Li, Y. Pei, *Thermally insulative thermoelectric argyrodites*, Materials Today., 48(2), 198 (2021); <https://doi.org/10.1016/j.mattod.2021.01.007>.
- [6] L. Gao, M.-H. Lee, J. Zhang, *Metal-cation substitutions induced the enhancement of second harmonic generation in A₈BS₆ (A = Cu, and Ag; B = Si, Ge, and Sn)*, New J. Chem., 43, 37193 (2019); <https://doi.org/10.1039/C8NJ06270F>.
- [7] C. Yu, F. Zhao, J. Luo, L. Zhang, X. Sun, *Recent development of lithium argyrodite solid-state electrolytes for solid-state batteries: Synthesis, structure, stability and dynamics*, Nano Energy., 83, 105858 (2021); <https://doi.org/10.1016/j.nanoen.2021.105858>.
- [8] K.-W. Cheng, W.-T. Tsai, Y.-H. Wu, *Photo-enhanced salt-water splitting using orthorhombic Ag₈SnS₆ photoelectrodes in photoelectrochemical cells*, Journal of Power Sources., 317, 81 (2016); <https://doi.org/10.1016/j.jpowsour.2016.03.086>.
- [9] I.Y. Nekrasov, M.P. Kulakov, Z.D. Sokolovskaya, A.V. Chichagov, *Phase relations in the tin-silver systems Ag₂S–SnS and Ag₂S–SnS₂*, Geochem. Int., 13, 23 (1976).
- [10] O. Gorochov, *Les composés Ag₈MX₆ (M=Si, Ge, Sn et X=S, Se, Te)*, Bull. Soc. Chim. France, 6, 2263 (1968).
- [11] O.V. Parasyuk, I.D. Oleksyuk, L.V. Piskach, S.V. Volkov, V.I. Pekhnyo, *Phase relations in the Ag₂S–CdS–SnS₂ system and the crystal structure of the compounds*, J. Alloys Compd., 399(1-2), 173 (2005); <https://doi.org/10.1016/j.jallcom.2005.03.023>.
- [12] C.-L. Lu, L. Zhang, Y.-W. Zhang, S.-Y. Liu, Y. Mei, *Electronic, optical properties, surface energies and work functions of Ag₈SnS₆: First-principles method*, Chin. Phys. B., 24(1), 017501 (2015); <https://doi.org/10.1088/1674-1056/24/1/017501>.
- [13] X. Shen, Y. Xia, C.-C. Yang, Z. Zhang, S. Li, Y.-H. Tung, A. Benton, X. Zhang, X. Lu, G. Wang, J. He, X. Zhou, *High Thermoelectric Performance in Sulfide-Type Argyrodites Compound Ag₈Sn(S_{1-x}Se_x)₆ Enabled by Ultralow Lattice Thermal Conductivity and Extended Cubic Phase Regime*, Advanced Functional Materials., 30(21), 2000526 (2020); <https://doi.org/10.1002/adfm.202000526>.
- [14] T.J. Slade, V. Gvozdetzkyi, J.M. Wilde, A. Kreyssig, E. Gati, L.-L. Wang, Y. Mudryk, R.A. Ribeiro, V.K. Pecharsky, J.V. Zaikina, S.L. Bud'ko, P.C. Canfield, *A Low-Temperature Structural Transition in Canfieldite, Ag₈SnS₆, Single Crystals*, Inorg. Chem., 60(24), 19345 (2021); <https://doi.org/10.1021/acs.inorgchem.1c03158>.
- [15] C. Sturm, N. Boccalon, D. Ramirez, H. Kleinke, *Stability and Thermoelectric Properties of the Canfieldite Ag₈SnS₆*, ACS Appl. Energy Mater. 4(9), 10244 (2021); <https://doi.org/10.1021/acsapem.1c02118>.
- [16] Wang N. *New data for Ag₈SnS₆ (canfieldite) and Ag₈GeS₆ (argyrodite)*, Neues Jahrb. Mineral. Monatsh., 269 (1978).
- [17] O. Gorochov, *Les composés Ag₈MX₆ (M=Si, Ge, Sn et X=S, Se, Te)*, Bull. Soc. Chim. France., 6, 2263 (1968).
- [18] G.H. Moh, *Experimental and descriptive ore mineralogy. the Ag–Sn–S system. the Ag–Ge–S system*, N. Jb. Miner. Abh., 128(2), 146 (1976).

- [19] Z.M. Aliyeva, S.M. Bagheri, Z.S. Aliev, I.J. Alverdiyev, Y.A. Yusibov, M.B. Babanly, *The phase equilibria in the Ag₂S–Ag₈GeS₆–Ag₈SnS₆ system*, J. Alloys Compd., 611, 395 (2014); <https://doi.org/10.1016/j.jallcom.2014.05.112>.
- [20] A. Sugaki, A. Kitakaze, H. Kitazawa, Science Reports of the Tohoku University, Series III, 16(2), 199 (1985).
- [21] J.P. Perdew, K. Burke, and M. Ernzerhof, *Generalized Gradient Approximation Made Simple*, Phys. Rev. Lett., 78(7), 1396 (1997); <http://dx.doi.org/10.1103/physrevlett.78.1396>.
- [22] J.P. Perdew, A. Ruzsinszky, G.I. Csonka, O.A. Vydrov, G.E. Scuseria, L.A. Constantin, B.K. Zhou, *Restoring the Density-Gradient Expansion for Exchange in Solids and Surfaces*, Phys. Rev. Lett., 100(13), 136406 (2008); <https://doi.org/10.1103/PhysRevLett.100.136406>.
- [23] H.J. Monkhorst, J.D. Pack, *Special points for Brillouin-zone integrations*, Phys. Rev. B., 13(12), 5188 (1976); <https://doi.org/10.1103/PhysRevB.13.5188>.
- [24] C.W.F.T. Pistorius, O. Gorochov, *Polymorphism and stability of the semiconducting series Ag₈MX₆ (M = Si, Ge, Sn, i X = S, Se, Te) to high pressures*, High Temperatures- High Pressures., 2(1), 31 (1970).
- [25] A. Kindurys, A. Shileika, *Investigations of the absorption edge of the compounds at phase transitions*, Inst. Phys. Conf. Ser., 35, 67 (1977).
- [26] L. Wang, W. Wang, *A New Strategy to Design Highly Sustainable Sulfide PhotoCatalyst for Hydrogen Production*, Chinese Journal of Chemistry, 35(2), 148 (2017); <https://doi.org/10.1002/cjoc.201600668>.
- [27] H.A. Ilchuk, L.I. Nykyruy, A.I. Kashuba, I.V. Semkiv, M.V. Solovyov, B.P. Naidych, V.M. Kordan, L.R. Deva, M.S. Karkulovska, R.Y. Petrus, *Electron, phonon, optical and thermodynamic properties of CdTe crystal calculated by DFT*, Physics and Chemistry of Solid State., 23(2), 261 (2022); <https://doi.org/10.15330/pcss.23.2.261-269>.
- [28] A. Kashuba, *Influence of metal atom substitution on the electronic and optical properties of solid-state Cd_{0.75}X_{0.25}Te (X= Cu, Ag and Au) solutions*, Physics and Chemistry of Solid State., 24(1), 92 (2023); <https://doi.org/10.15330/pcss.24.1.92-101>.
- [29] W. Kohn, L. J. Sham, *Self-Consistent Equations Including Exchange and Correlation Effects*, Phys. Rev. A., 140(4), 1133 (1965); <https://doi.org/10.1103/PhysRev.140.A1133>.
- [30] I.V. Semkiv, B.A. Lukiyanets, H.A. Ilchuk, R.Yu. Petrus, A.I. Kashuba, M.V. Chekaylo, *Energy Structure of β'-phase of Ag₈SnSe₆ Crystal*, J. Nano- Electron. Phys., 8(1), 01011 (2016); [http://dx.doi.org/10.21272/jnep.8\(1\).01011](http://dx.doi.org/10.21272/jnep.8(1).01011).
- [31] M.Ya. Rudysh, M.G. Brik, V.Yo. Stadnyk, R.S. Brezvin, P.A. Shchepanskyi, A. Fedorchuk, O.Y. Khyzhun, I.V. Kityk, M. Piasecki, *Ab initio calculations of the electronic structure and specific optical features of β-LiNH₄SO₄ single crystals*, Physica B Condens, 528, 37 (2018); <https://doi.org/10.1016/j.physb.2017.10.085>.
- [32] M.Ya. Rudysh, P.A. Shchepanskyi, A.O. Fedorchuk, M.G. Brik, C.-G. Ma, G.L. Myronchuk, M. Piasecki, *First-principles analysis of physical properties anisotropy for the Ag₂SiS₃ chalcogenide semiconductor*, J. Alloys Compd., 826, 154232 (2020); <https://doi.org/10.1016/j.jallcom.2020.154232>.
- [33] A. Fonari, C. Sutton, *Effective Mass Calculator* (2012). <https://github.com/afonari/emc>.

I.V. Семків¹, Г.А. Ільчук¹, Н.Ю. Кашуба¹, В.М. Кордан², А.І. Кашуба¹

Синтез, кристалічна та енергетична структура кристалу Ag₈SnS₆

¹Національний університет “Львівська політехніка”, Львів, Україна,
e-mail: ihor.v.semkiv@lpnu.ua

²Львівський національний університет імені Івана Франка, Львів, Україна

Кристал Ag₈SnS₆ було вирощено шляхом прямого плавлення високочистої стехіометричної суміші елементарних Ag, Sn та S у герметичній кварцовій ампулі. Даний аргіродит кристалізується в орторомбичній структурі (просторова група Pna2₁ (№ 33)) при кімнатній температурі. Проведено першопринципні розрахунки електронної зонної структури та густини станів кристала α'-Ag₈SnS₆ з використанням узагальненого градієнтного наближення (GGA) і наближення локальної щільності (LDA). Функціонал Пердью–Берка–Ернзерхофа (PBE) та PBEsol було застосовано для GGA розрахунків. Усі розраховані характеристики добре корелюють з наявними експериментальними даними. На основі електронної зонної структури розраховано ефективну масу електронів і дірок. Обговорюється анізотропна поведінка електронної зонної структури.

Ключові слова: аргіродит, синтез, X-променева дифракція, морфологія, теорія функціонала густини, зонна структура, ефективна маса, щільність станів.